



**EXPERIMENTAL REVIEW ON QUARKONIUM**

Vaia Papadimitriou

*Fermilab, P.O. Box 500, Batavia, IL, 60510, U.S.A.*

Presenting results from the  
FNAL, HERA, KEKB, PEP-II and LEP-II experiments at  
Les Rencontres de Physique de la Vallée d'Aoste, 29 Feb.-6 Mar. 2004

Abstract

We discuss current issues and present the latest measurements on quarkonia production and spectroscopy from experiments monitoring hadron-hadron, lepton-hadron and lepton-lepton collisions. These measurements include cross section and polarization results for charmonium and bottomonium states. We also discuss the discovery and properties of the yet unexplained narrow state  $X(3872)$ .

## 1 Introduction

The study of quarkonia has yielded valuable insight into the nature of strong interactions since the discovery of the  $J/\psi$  in 1974. Heavy quarkonia states,  $c\bar{c}$  and  $b\bar{b}$ , provide very useful systems for the study of both perturbative and non perturbative QCD. As far as the strong interactions are concerned, heavy quarkonia are the next simplest particles (probes) after leptons and electroweak gauge bosons. In addition, the charmonium and bottomonium systems exhibit a rich spectrum of orbital and angular excitations and therefore they can potentially provide more information than leptons and electroweak gauge bosons.

The experimental results reported in this review come from  $p\bar{p}$  collisions at  $\sqrt{s} = 1.96(1.8)$  TeV (CDF and D0 experiments at Fermilab); from collisions of 800 GeV protons with a fixed target (E866 experiment at Fermilab); from  $e^\pm p$  collisions at  $\sqrt{s} = 319(301)$  GeV (H1 and Zeus experiments at DESY); from collisions of 920 GeV protons with a fixed target (HERA-B experiment at DESY); from  $e^+e^-$  collisions at  $\sqrt{s} = 10.6$  GeV (BaBar experiment at PEP-II and Belle experiment at KEKB) and from  $e^+e^-$  collisions at  $\sqrt{s} = 197$  GeV (DELPHI experiment at LEP-II).

This paper is organized as follows. In section 2 we describe results on production, in section 3 we describe results on spectroscopy and in section 4 we discuss conclusions and prospects.

## 2 Results on Production

### 2.1 Results from the CDF and D0 experiments

The Fermilab Tevatron has operated in the past several years either in a collider mode or in a fixed target mode. In the collider mode 900(980) GeV/c protons collide with antiprotons of the same energy, while in the fixed target mode 800 GeV protons hit a fixed target.

From August 1992 to February 1996 (Run I) the CDF and D0 detectors collected data samples, approximately  $110 pb^{-1}$  each, of  $p\bar{p}$  collisions at  $\sqrt{s} = 1.8$  TeV. In Run I the crossing time was  $3.5 \mu s$  for 6 bunches and the typical luminosity of order  $10^{31} cm^{-2}sec^{-1}$ . Run II physics quality data started in March 2002. By July 2004, approximately  $550 pb^{-1}$  of data at  $\sqrt{s} = 1.96$  TeV were delivered to each of the two upgraded detectors. In Run II the crossing time is 396 ns for 36 bunches and the typical luminosity so far of order  $8 \times 10^{31} cm^{-2}sec^{-1}$ .

#### 2.1.1 Cross sections

The CDF collaboration has previously reported results on the production of  $J/\psi$  and  $\psi(2S)$  mesons <sup>1, 2</sup>. The measured cross sections for direct produc-

tion were of the order of 50 times larger than predicted by the Color Singlet Model (CSM) <sup>3)</sup>. However calculations based on the NRQCD factorization formalism <sup>4, 5)</sup> are able to account for the observed cross sections for  $p_T > 5$  GeV/c by including color octet production mechanisms.

Using Run I data CDF has also reported <sup>6)</sup> production cross section results of inclusive  $\Upsilon(1S)$ ,  $\Upsilon(2S)$  and  $\Upsilon(3S)$  states in the region  $0 < p_T < 20$  GeV/c. In addition, it has reported <sup>7)</sup> on the fraction of  $\Upsilon(1S)$  mesons originating from  $\chi_b(1P)$ ,  $\chi_b(2P)$ ,  $\chi_b(3P)$ ,  $\Upsilon(2S)$ ,  $\Upsilon(3S)$  and from direct production for  $p_T^x > 8$  GeV/c. The rate of inclusive  $\Upsilon$  production for all three states was found to be higher than color-singlet QCD calculations by a factor of about 5 for  $p_T > 4$  GeV/c. Inclusion of color-octet production mechanisms within the NRQCD framework can account for the observed cross section for  $p_T > 8$  GeV/c. The theoretical prediction for the cross sections diverges at low  $p_T$  while the data turn over and approach zero <sup>5, 8)</sup>.

The amplitude for each  $c\bar{c}$  or  $b\bar{b}$  state with definite colour and angular momentum factorizes into a short distance term which can be calculated in NRQCD and a long distance matrix element (LDME) describing the transition to a bound quarkonium state. The LDMEs are not calculable and have been determined from Tevatron data where the Color Octet contributions were found to be sizable. These matrix elements are expected to be universal and can in principle be used in the theoretical predictions for HERA and LEP results.

At large transverse momenta, fragmentation type production is expected to dominate and color-octet matrix elements dominate the color-singlet matrix element contribution. At low transverse momenta, soft gluon effects and non-fragmentation effects from other octet matrix elements, that are difficult to calculate theoretically, become important and cause theory predictions and data to diverge (see discussion above on the CDF  $\Upsilon$  data). The Run-II CDF detector has an improved dimuon trigger with a lower  $p_T$  threshold of  $> 1.4$  GeV/c. This has extended the low transverse momentum range of triggered  $J/\psi$ ,  $\psi(2S) \rightarrow \mu\mu$  events down to  $p_T(\mu\mu) \geq 0$  GeV/c.

Using a  $39.7 \text{ pb}^{-1}$  data sample from Run II, the CDF Collaboration has measured the inclusive cross section for  $J/\psi$  production and subsequent decay into  $\mu^+\mu^-$  <sup>9)</sup>. The inclusive cross section includes both prompt  $J/\psi$ 's and  $J/\psi$ 's from decays of  $b$ -hadrons. The inclusive differential cross section multiplied by the branching fraction for  $J/\psi \rightarrow \mu^+\mu^-$  has been obtained down to zero transverse momentum and is shown in the left panel of fig. 1 as a function of  $p_T$  for rapidity  $|y| < 0.6$ . The total integrated cross section for inclusive  $J/\psi$  production in  $p\bar{p}$  interactions at  $\sqrt{s} = 1.96$  TeV is measured to be

$$\sigma[p\bar{p} \rightarrow J/\psi X, |y(J/\psi)| < 0.6] = 4.08 \pm 0.02(\text{stat}) \pm 0.36(\text{syst}) \mu\text{b}. \quad (1)$$

These new measurements await comparison with updated theoretical calculations in the low  $p_T$  region.

Using a sample of  $4.7 \text{ pb}^{-1}$  of Run II data the D0 collaboration has verified that the  $J/\psi$  cross section is independent of the rapidity of the  $J/\psi$  for a rapidity range between  $0 < |y| < 2$ . This analysis has been performed for  $p_T(J/\psi) > 5 \text{ GeV}/c$  and  $p_T(J/\psi) > 8 \text{ GeV}/c$  <sup>10)</sup>.

Using  $39.7 \text{ pb}^{-1}$  of the Run II data, the CDF Collaboration has also measured the differential cross section for  $b$ -hadrons in the decay channel  $H_b \rightarrow J/\psi X$  as a function of  $p_T$ , as well as the cross section integrated over  $p_T$  <sup>9)</sup>. The differential cross section multiplied by the branching fraction for  $J/\psi \rightarrow \mu^+ \mu^-$  is shown in the right panel of fig. 1. A recent QCD theoretical calculation using a fixed order (FO) calculation with resummation of next-to-leading order logs (NLL) <sup>11)</sup> is overlaid. The cross section integrated over  $p_T$  was found to be

$$\sigma[p\bar{p} \rightarrow H_b X, p_T(J/\psi) > 1.25 \text{ GeV}/c, |y(J/\psi)| < 0.6] = 28.4 \pm 0.4(\text{stat})_{-3.8}^{+4.0}(\text{syst}) \mu\text{b}. \quad (2)$$

The total single  $b$ -quark cross section integrated over one unit of rapidity was found to be

$$\sigma(p\bar{p} \rightarrow bX, |y| < 0.6) = 17.6 \pm 0.4(\text{stat})_{-2.3}^{+2.5}(\text{syst})\mu\text{b} \quad (3)$$

where  $b$  denotes either  $b$ -hadron states or  $\bar{b}$ -hadron states such that  $\sigma(p\bar{p} \rightarrow bX) = 1/2 \times \sigma(p\bar{p} \rightarrow H_b X)$ .

Using  $159.1 \text{ pb}^{-1}$  of the Run II data, the D0 Collaboration has measured <sup>12)</sup> the  $\Upsilon(1S)$  differential cross section as a function of transverse momentum and for three different ranges of rapidity of the  $\Upsilon(1S)$ :  $0 < |y^\Upsilon| < 0.6$ ,  $0.6 < |y^\Upsilon| < 1.2$  and  $1.2 < |y^\Upsilon| < 1.8$ . As can be seen from the left panel of fig. 2, the shapes of  $d\sigma/dp_T$  show little variation with rapidity. They are also consistent with the published Run I CDF measurement.

Using Run I data CDF has measured <sup>2)</sup> as well the fraction of  $J/\psi$  mesons originating from  $\chi_c$  meson decays. In addition, it has measured <sup>13)</sup> the relative rate of production of the charmonium states  $\chi_{c1}$  and  $\chi_{c2}$  through their decay into  $J/\psi\gamma$  where the photon from the decay is reconstructed through conversion into  $e^+e^-$  pairs. This makes the resolution of the two states possible. The CDF result appears to prefer an approximately equal production of the two  $\chi_{cJ}$  states, although it is consistent with the expectation that the cross sections are proportional to  $(2J+1)$  at high  $p_T(\chi_{cJ})$ . Both the CDF and D0 collaborations are pursuing these analyses further with Run II data. In the right panel of fig. 2 we show the charmonium states  $\chi_{c1}$  and  $\chi_{c2}$  reconstructed from a sample of  $114 \text{ pb}^{-1}$  of Run II data collected with the D0 detector <sup>10)</sup>. These states are

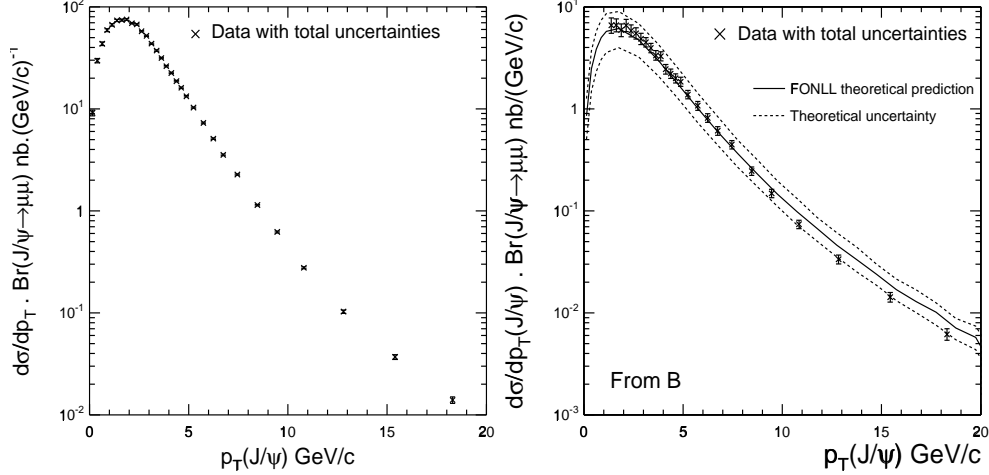


Figure 1: *Differential inclusive cross section for  $p\bar{p} \rightarrow J/\psi X$  (left). Differential cross section distribution of  $J/\psi$  events from  $b$ -hadron decay (right). Both cross sections are plotted as a function of the transverse momentum  $p_T$  of the  $J/\psi$  and are integrated over the rapidity range  $|y(J/\psi)| < 0.6$ .*

observed via their decays into  $J/\psi\gamma$  where the photon is reconstructed through conversions.

CDF has also searched for the  $\eta_b(1S)$  state via the  $\eta_b \rightarrow J/\psi J/\psi$ ;  $J/\psi \rightarrow \mu\mu$  decay channel using approximately  $100 \text{ pb}^{-1}$  of Run I data. A small cluster of 7 events was observed in the search window of 9.36 to 9.46  $\text{GeV}/c^2$  while 1.8 background events were expected. The probability that the background could mimic the data was assessed to be 1.5%. A simple fit to the mass of the cluster gave  $9455 \pm 6(\text{stat}) \text{ MeV}/c^2$ . Since the cluster of events was small, a 95% C.L. upper limit on  $\sigma_{\eta_b}(|y| < 0.4) Br(\eta_b \rightarrow J/\psi J/\psi) [Br(J/\psi \rightarrow \mu\mu)]^2$  was calculated, yielding 18 pb with an 11% relative systematic uncertainty. Run II data will be used to repeat this search and improve the limit or make an observation.

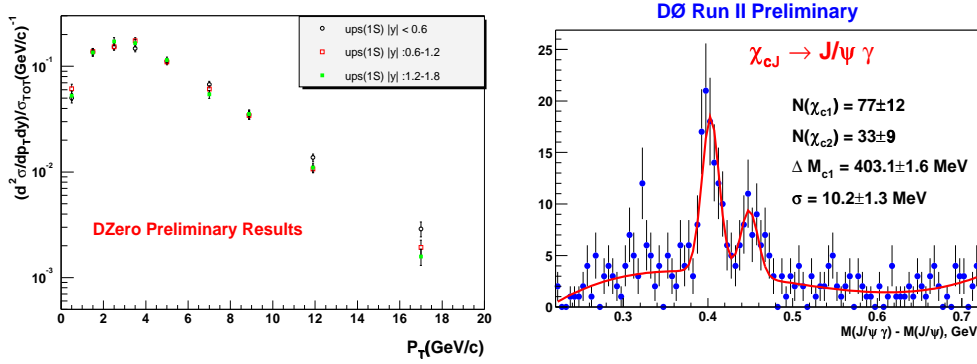


Figure 2: Normalized differential inclusive  $\Upsilon(1S)$  cross section in different rapidity regions (left). The  $M(J/\psi\gamma) - M(J/\psi)$  distribution from Run II DØ data. The  $\chi_{c1}$  and  $\chi_{c2}$  states are observed via their decays into  $J/\psi\gamma$  where the photon is reconstructed through conversions into  $e^+e^-$  pairs (right).

### 2.1.2 Polarization

Within NRQCD [4, 5] it is predicted that directly produced  $J/\psi$ ,  $\psi(2S)$  or  $\Upsilon$  mesons will be increasingly transversely polarized at high  $p_T$ .

CDF has measured with Run I data the polarization of the  $J/\psi$ ,  $\psi(2S)$  and  $\Upsilon(1S)$  states decaying into two muons. The muons from the decay of the above mesons are assumed to have an angular distribution proportional to  $1 + \alpha \cos^2(\theta^*)$  where  $\theta^*$  is the polar angle in the rest frame of the meson. The variable  $\alpha$  is defined as  $\alpha = (\sigma_T - 2\sigma_L)/(\sigma_T + 2\sigma_L)$  where  $\sigma_T$  and  $\sigma_L$  are the cross sections for transversely and longitudinally polarized states respectively and can vary between  $\pm 1$ . Unpolarized mesons have  $\alpha = 0$ , while  $\alpha = +1$  or  $-1$  correspond to fully transverse or longitudinal polarizations respectively.

CDF has measured the  $J/\psi$  and  $\psi(2S)$  polarizations using 110  $\text{pb}^{-1}$  of Run I data and the  $\Upsilon(1S)$  polarization using 77  $\text{pb}^{-1}$  of Run I data. In fig. 3 (left)

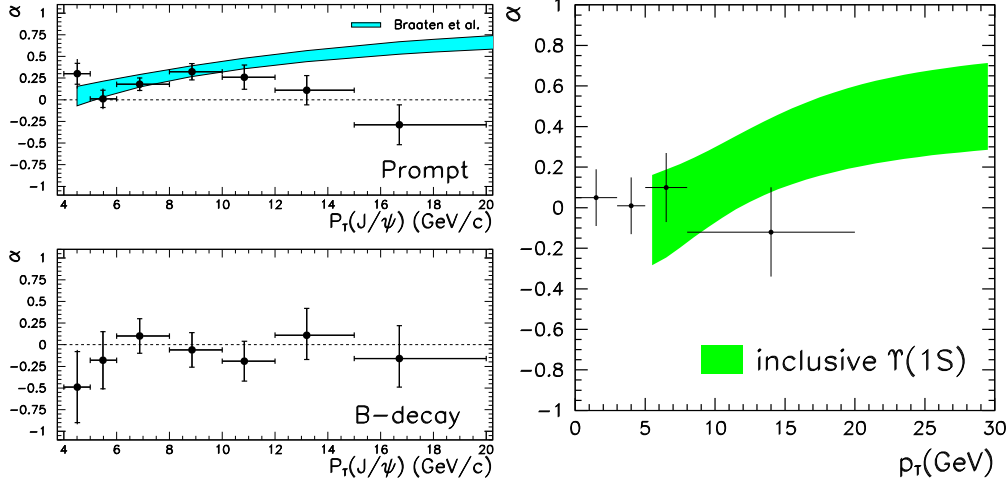


Figure 3: Polarization variable  $\alpha$  for inclusive  $J/\psi$  mesons from prompt production and  $B$ -hadron decay. The shaded band shows an NRQCD prediction<sup>15)</sup> which includes the contribution from  $\chi_c$  and  $\psi(2S)$  decays (left). Polarization variable  $\alpha$  for inclusive  $\Upsilon(1S)$  states from CDF Run I data as a function of  $\Upsilon(1S)$   $p_T$ . The theoretical band represents the NRQCD prediction<sup>16)</sup> (right).

we show the measurement<sup>14)</sup> of the polarization variable  $\alpha$  for prompt  $J/\psi$ 's and for  $J/\psi$ 's originating from  $B$  decays. These polarization measurements at  $\sqrt{s} = 1.8$  TeV indicate that the polarization from  $B$  decays is generally consistent with zero, as expected. In both the  $J/\psi$  and  $\psi(2S)$  cases, CDF does not observe increasing prompt transverse polarization for  $p_T \geq 12$  GeV/c. Although the measurements are limited by statistics, especially the  $\psi(2S)$ , they appear to indicate that no large transverse prompt polarization is present at high  $p_T$ , in disagreement with NRQCD factorization predictions.

In fig. 3 (right) we show the measurement<sup>6)</sup> of the polarization variable  $\alpha$  for inclusive  $\Upsilon(1S)$ .  $\alpha$  is predicted to be small for  $p_T$  less than 10 GeV/c but is increasing steadily with  $p_T$ . The prediction is compatible with the CDF

measurement of  $\alpha = 0.03 \pm 0.28$  for  $p_T$  in the range from 8 GeV/c to 20 GeV/c. The  $\Upsilon(1S)$  data are consistent with unpolarized production in the region  $0 < p_T < 20$  GeV/c. Although the Run I CDF data did not provide sufficient information for  $p_T > 20$  GeV/c, this should be possible with Run II data. In Run II it should be also possible to measure the polarizations of the  $\Upsilon(2S)$  and  $\Upsilon(3S)$  states. This would be particularly interesting in view of the  $\Upsilon$  polarization measurements from the fixed target Fermilab experiment E866 discussed in section 2.2.

## 2.2 Results from the E866/NuSea experiment

The E866/NuSea experiment ran for a period of approximately six months during 1996-1997 in the Fermilab Meson-East area at an energy of  $\sqrt{s} = 38.8$  GeV.

The E866 experiment has studied the production of dimuons in the collision of 800 GeV/c protons with a copper beam dump. Among other interesting results, they derived <sup>17)</sup> polarizations from the angular distribution of 2 million dimuons in the range  $8.1 < m_{\mu^+\mu^-} < 15.0$  GeV. The data cover the kinematic range  $0.0 < x_F < 0.6$  and  $p_T < 4.0$  GeV/c. In fig. 4 we show the polarization variable  $\alpha$  as a function of  $p_T$  and  $x_F$ . The  $\Upsilon(1S)$  data show almost no polarization at small  $x_F$  and  $p_T$ . The data show a finite transverse polarization at either large  $p_T$  or large  $x_F$ . This observation disagrees with an NRQCD calculation that predicts a polarization in the range of 0.8-0.31 (averaged over  $x_F$  and  $p_T$ ) for these energies <sup>18)</sup>. A fit to the  $\Upsilon(1S)$  state for a polarization independent of  $x_F$  and  $p_T$  gives  $\alpha = 0.07 \pm 0.04$ . The observation that the polarization of the cross-section-weighted average of the  $\Upsilon(2S+3S)$  states is much larger than that of the  $\Upsilon(1S)$  state at all  $x_F$  and  $p_T$  contrasts sharply with what is seen in the charmonium system <sup>14)</sup>.

## 2.3 Quarkonium production at LEP

The LEP collider was used to study  $e^+e^-$  collisions at the  $Z^0$  resonance. Charmonium was produced at LEP through direct production in  $Z^0$  decay, through the decay of  $b$ -hadrons and through  $\gamma\gamma$  collisions. The ALEPH, DELPHI, L3 and OPAL collaborations have measured the inclusive branching fractions into prompt  $J/\psi$  <sup>19, 20, 21, 22)</sup>.

The inclusive cross section of  $\gamma\gamma \rightarrow J/\psi X$  at LEP II has been measured by the DELPHI Collaboration <sup>23, 24)</sup>. The results of a LO theoretical computation <sup>25)</sup> which uses the NRQCD matrix elements of Ref. <sup>15)</sup> is compared to the data. As can be seen from fig. 5, the data-theory comparison clearly favors that NRQCD-factorization approach over the color-singlet model.

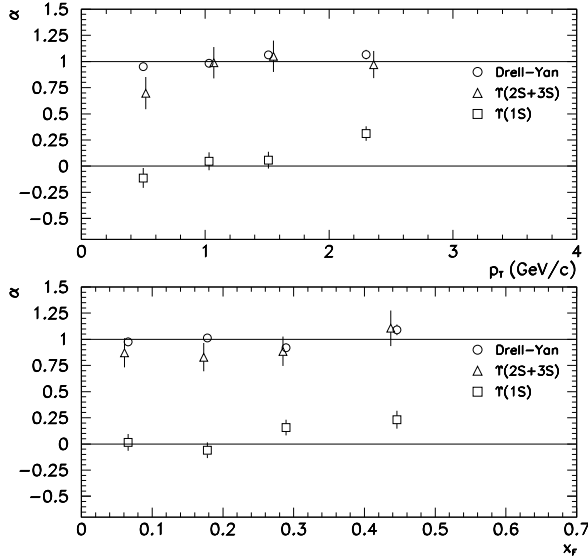


Figure 4:  $\alpha$  vs  $p_T$  for the Drell-Yan sidebands and the  $\Upsilon(1S)$  and  $\Upsilon(2S+3S)$  regions (top).  $\alpha$  vs  $x_F$  for the same mass regions (bottom). The errors shown are statistical; there is an additional systematic error in  $\alpha$  (not shown) of 0.02 for Drell-Yan polarizations and 0.06 for quarkonium polarizations.

#### 2.4 Results from the H1 and Zeus experiments

At the HERA storage ring at DESY, electrons or positrons of 27.6 GeV and protons of 920 GeV (820 GeV before 1998) collide resulting in a center of mass energy  $\sqrt{s}$  of 319 GeV (301 GeV). The HERA I running period ended in September 2000 after having delivered to the H1 and Zeus experiments over  $100 \text{ pb}^{-1}$  of data.

The production of  $J/\psi$  mesons,  $ep \rightarrow eJ/\psi X$ , has been studied intensively at HERA. In  $ep$  collisions quarkonia are predominantly produced via the photon gluon fusion mechanism, where a photon emitted by the incoming electron interacts with a gluon in the proton forming a quark-antiquark pair. The high available energy allows the contributing mechanisms to be studied in a wide kinematic range in both  $Q^2$  and  $W_{\gamma p}$ , where  $Q^2$  is the negative squared four-momentum of the exchanged photon and  $W_{\gamma p}$  is the center of mass energy of the

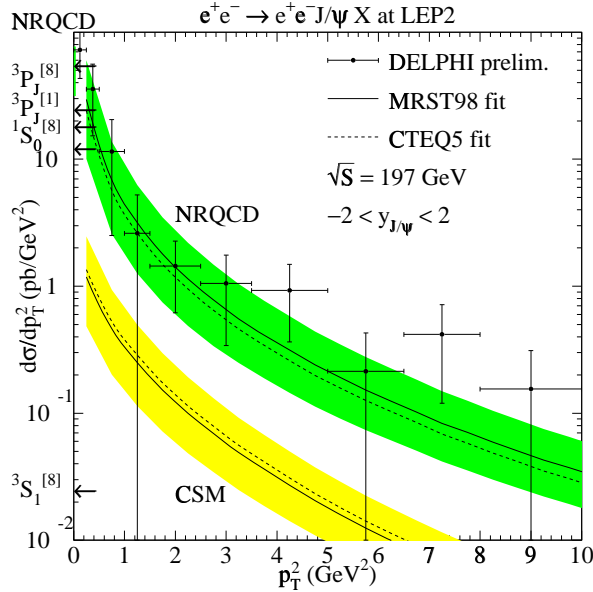


Figure 5: *Differential cross section for the process  $\gamma\gamma \rightarrow J/\psi X$  as a function of  $p_T^2$ . The data points are from the DELPHI Collaboration. The upper set of curves is the NRQCD factorization predictions and the lower set of curves represents the color-singlet model. The solid and dashed curves correspond to the MRST98LO and CTEQ5L parton distributions, respectively.*

photon-proton system. The major contribution in this production mechanism is due to the exchange of almost real photons corresponding to a photon virtuality  $Q^2 \approx 0$  (photoproduction). In deep inelastic scattering (DIS)  $Q^2$  is large, often defined experimentally by  $Q^2 > 2 \text{ GeV}^2$ .

Previous HERA measurements on quarkonia production show good agreement with the colour singlet model (CSM), but small colour octet contributions could not be ruled out.

Recent results on photoproduction and in a large kinematic region from H1 <sup>26)</sup> and Zeus <sup>27)</sup> are shown in fig. 6. Photon-proton cross sections  $\sigma_{\gamma p}$ ,  $d\sigma/dz$  and  $d\sigma/dp_{T,\psi}^2$  are shown in the range  $0.3 < z < 0.9$  where  $z$  is the fraction of the photon energy transferred to the  $J/\psi$  meson in the proton rest frame. There is good agreement between the two experiments. The data are

also well described by the NLO CSM calculations<sup>28)</sup>. In contrast, the LO calculation is too steep in  $p_{t,\psi}^2$ .

In fig. 7 we show the differential  $J/\psi$  cross section from photoproduction as a function of  $z$ . The distribution can be described in the full range of  $z$  by LO NRQCD calculations<sup>28)</sup>.

Inelastic electroproduction of  $J/\psi$  mesons<sup>26)</sup> is studied in the region  $2 < Q^2 < 100 \text{ GeV}^2$  for  $0.3 < z < 0.9$  and for  $p_{t,\psi}^{*2} > 1 \text{ GeV}^2$ , where  $p_{t,\psi}^{*2}$  is the squared transverse momentum of the  $J/\psi$  meson in the photon-proton center of mass system. In fig. 8 we show the differential  $J/\psi$  electroproduction cross section from H1 as a function of  $Q^2$  and  $p_{t,\psi}^{*2}$  along with the theoretical calculations. The bands include the theoretical uncertainties originating from the uncertainty in the charm quark mass, the variation of renormalization and factorization scales by factors 1/2 and 2, and the errors of the NRQCD matrix elements<sup>15)</sup>. Neither the full NRQCD calculation<sup>29)</sup> nor the colour singlet part can describe the data in normalization over the full range. A high  $Q^2$  and  $p_{t,\psi}^{*2}$  agreement with the full NRQCD calculation is found.

## 2.5 Results from the HERA-B experiment

The HERA-B experiment operated at the HERA ring as a fixed target experiment. It studied charmonium and other heavy flavor states by inserting wire targets into the halo of the 920 GeV proton beam circulating in the ring. In the period November 2002- February 2003 HERA-B has collected about  $150 \times 10^6$  events with a di-lepton trigger. The main goal was to study the charmonium production in pA collisions at  $\sqrt{s} = 41.6 \text{ GeV}$  with different materials.

One of the interesting measurements they have made is of the fraction of  $J/\psi$ 's produced via radiative  $\chi_c$  decays in interactions of 920 GeV protons with carbon and titanium targets. Using the 2000 data and averaging over all types of collisions they obtained  $R_{\chi_c} = 0.32 \pm 0.06(\text{stat}) \pm 0.04(\text{sys})$ . In fig. 9 we show the measurement of  $R_{\chi_c}$  from the HERA-B experiment in comparison with similar measurements from other fixed target experiments. The HERA-B result is compatible with most of the previous data. Due to the relatively large uncertainties, a flat energy dependence as predicted by CEM cannot be ruled out. NRQCD predicts relatively well the slope of the energy dependence although its absolute predictions fall below most of the data. Similarly, the CSM predictions fall above most of the data. Although the corresponding CDF Run I measurement<sup>2)</sup> at  $\sqrt{s} = 1.8 \text{ TeV}$  is not shown in this plot, interestingly enough, it is consistent with the HERA-B measurement. Using a fraction of the 2002/2003 data, and in particular the dimuon channel to identify the  $J/\psi$ 's, the HERA-B Collaboration obtained a preliminary result of  $R_{\chi_c} = 0.21 \pm 0.05(\text{stat})$ . An updated measurement using the complete data sample would be very informative.

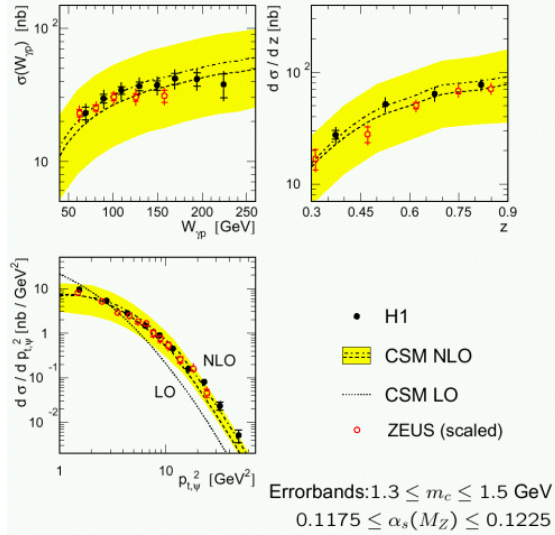


Figure 6: Total  $J/\psi$  photoproduction cross section as a function of  $W_{\gamma p}$  and differential cross sections as a function of  $z$  and  $p_{t,\psi}^2$ . The Zeus points are shifted by up to 12% to account for differences in the covered kinematic range. The CSM calculation in NLO is also shown and seems to be reproducing the shape of the data. The uncertainty in the theoretical calculations is shown by a band including normalization uncertainties due to the value of  $\alpha_s$  and the charm mass.

## 2.6 Quarkonium production in $e^+e^-$ annihilations at 10.6 GeV

The  $B$  factories have proved to be a rich source of data on charmonium production in  $e^+e^-$  annihilation. The Belle and BaBar collaborations have measured the inclusive cross section  $\sigma[e^+e^- \rightarrow J/\psi X]$  as well as the momentum distribution and angular distribution of the  $J/\psi$  (30, 31).

An interesting and surprising result from the Belle Collaboration is that most of the  $J/\psi$ 's that are produced in  $e^+e^-$  annihilation at  $\sqrt{s} = 10.6$  GeV are accompanied by charmed hadrons. A convenient measure of the probability

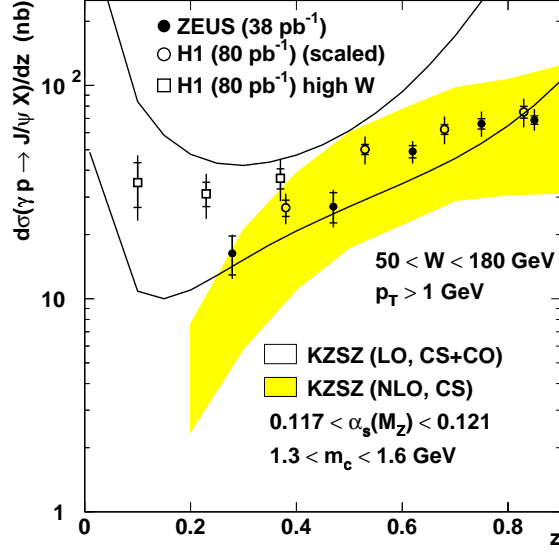


Figure 7: Differential  $J/\psi$  photoproduction cross section as a function of  $z$  for H1 and Zeus data and for  $p_T > 1$  GeV/c. The data is compared with predictions of the NLO colour singlet model and a prediction including both colour singlet and colour octet contributions in LO.

for creating a second  $c\bar{c}$  pair is the ratio

$$R_{double} = \frac{\sigma[e^+e^- \rightarrow J/\psi X_{c\bar{c}}]}{\sigma[e^+e^- \rightarrow J/\psi X]} \quad (4)$$

The Belle Collaboration finds that  $R_{double} = 0.82 \pm 0.15 \pm 0.14$  with  $R_{double} > 0.48$  at the 90% C.L. <sup>32)</sup>. On the other hand, the NRQCD factorization approach leads to the prediction  $R_{J/\psi} \approx 0.1$  <sup>33, 34, 35)</sup>. The discrepancy seems to arise primarily from the cross section in the numerator of equation (4) and its source remains a mystery.

There is also a large discrepancy between theory and experiment in an exclusive double- $c\bar{c}$  cross section. For the process  $e^+e^- \rightarrow J/\psi\eta_c$ , the Belle Collaboration measured <sup>32)</sup> the product of the cross section and the branching fraction for  $\eta_c$  to decay into at least four charged tracks to be  $46 \pm 6^{+7}_{-9}$  fb.

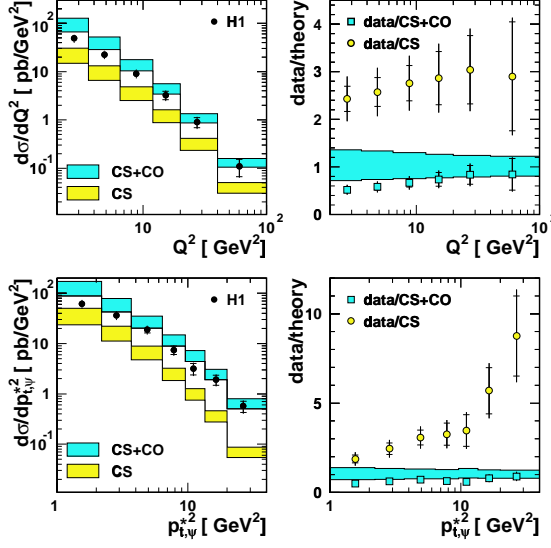


Figure 8: *Differential  $J/\psi$  electroproduction cross section as a function of  $Q^2$  and  $p_{t,\psi}^{*2}$ . The data are compared to a full NRQCD calculation<sup>29)</sup> (dark band) and to the LO colour singlet contribution alone (light band). Data over theory ratios are also presented.*

In contrast, LO calculations predict a cross section of  $2.31 \pm 1.09$  fb<sup>36, 37)</sup>. There are some uncertainties in the prediction from uncalculated higher-order corrections and from NRQCD matrix elements. Nevertheless, because this is an exclusive process, only color-singlet matrix elements enter, and those are well determined. In an attempt to provide at least a partial explanation for the discrepancy, it was suggested<sup>38)</sup> that processes proceeding via two virtual photons may be important and that the signal that was attributed to  $e^+e^- \rightarrow J/\psi\eta_c$  might also include  $J/\psi J/\psi$  events.

Using a data sample of  $140 \text{ fb}^{-1}$  collected at the  $\Upsilon(4S)$  resonance,  $152 \text{ M } \Upsilon(4S) \rightarrow B\bar{B}$  decays, the Belle Collaboration has measured<sup>39)</sup> the mass of the system recoiling against the reconstructed  $J/\psi$  (fig. 10). Clear peaks around the nominal  $\eta_c$  and  $\chi_{c0}$  masses are evident. Another significant peak around  $3.63 \text{ GeV}/c^2$  is identified as the  $\eta_c(2S)$ . The fit in fig. 10 includes all the known

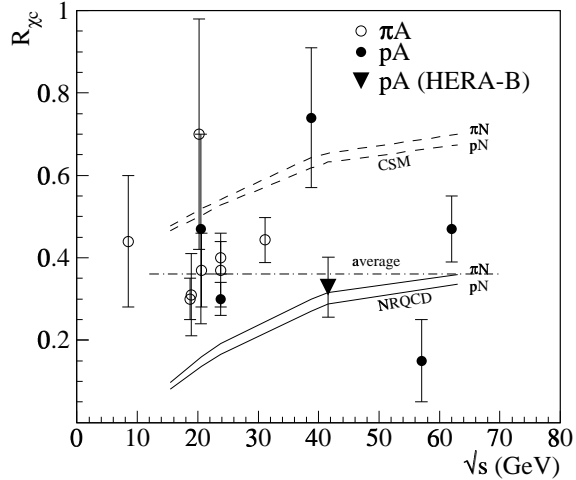


Figure 9: Comparison of the  $R_{\chi_c}$  HERA-B measurement (data of 2000) with those of other  $pp$ ,  $pA$ ,  $\pi p$  and  $\pi A$  experiments. The dot-dashed line is the average of all presented measurements. Also shown are predictions for  $pN$  and  $\pi N$  interactions obtained from Monte Carlo based on the CSM and NRQCD calculations. The Color Evaporation model (CEM) predicts a constant value.

narrow charmonium states. In this fit, the mass positions for the  $\eta_c$ ,  $\chi_{c0}$  and  $\eta_c(2S)$  are free parameters while those for  $J/\psi$ ,  $\chi_{c1}$ ,  $\chi_{c2}$  and  $\psi(2S)$  are fixed at their nominal values. The fit returns negative yield for the  $J/\psi$  and Belle has set an upper limit for  $\sigma(e^+e^- \rightarrow J/\psi J/\psi) \times B(J/\psi \rightarrow > 2 \text{ charged})$  of 9.1 fb at 90% C.L. This rules out the suggestion that a large fraction of the inferred  $J/\psi\eta_c$  signal consists of  $J/\psi J/\psi$  events.

### 3 Results on Spectroscopy

Over the past couple of years, experiments have established a number of new narrow states which have revitalized studies of the heavy quarkonium system. One of these states is the puzzling X(3872). This state is a charmonium candidate, the  $1^3D_2$  or  $1^3D_3$  or  $2^1P_1$  ( $h'_c$ ) or  $2^3P_1$  ( $\chi'_{c1}$ ) or  $1^3F_4$  states <sup>40, 41, 42</sup>,

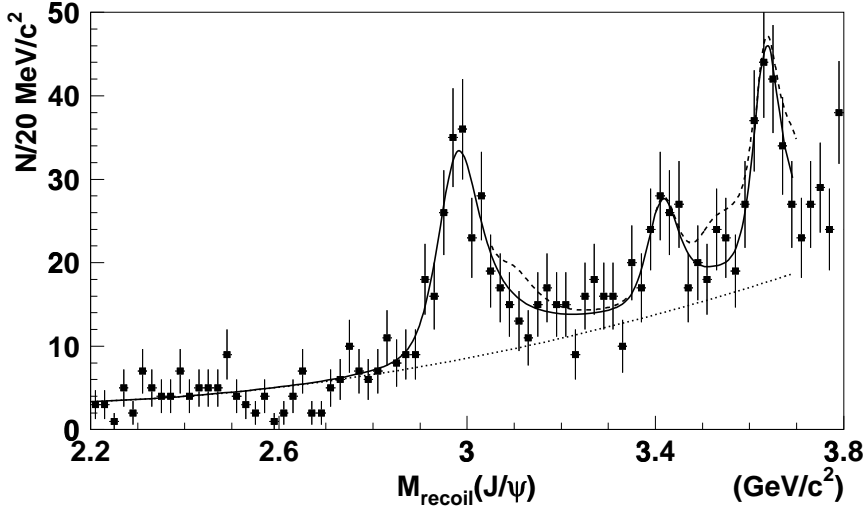


Figure 10: *The mass of the system recoiling against the reconstructed  $J/\psi$  in inclusive  $e^+e^- \rightarrow J/\psi X$  events.*

a candidate for a molecule of charmed  $D$  and  $D^*$  mesons<sup>43, 44, 45)</sup> or a candidate for a charmonium hybrid<sup>44, 46)</sup>.

### 3.1 The X(3872) State at Belle

Using  $140 \text{ fb}^{-1}$  of data, the Belle collaboration reported<sup>47)</sup> the observation of a narrow charmonium like state produced in the exclusive decay process  $B^\pm \rightarrow K^\pm \pi^+ \pi^- J/\psi$ . Fig. 11(a) shows the  $\Delta M \equiv M(\pi^+ \pi^- l^+ l^-) - M(l^+ l^-)$  distribution from the data. The large peak at  $0.589 \text{ GeV}$  corresponds to the  $\psi(2S) \rightarrow \pi^+ \pi^- J/\psi$  signal while the spike at  $\Delta M = 0.775 \text{ GeV}$  corresponds to  $35.7 \pm 6.8$  events of a new state with mass near  $3872 \text{ MeV}$ . Fig. 11(b) shows the same distribution for a large sample of generic  $B - \bar{B}$  Monte Carlo events where, except for the prominent  $\psi(2S)$  peak, the distribution is featureless. The new state, which decays to  $J/\psi \pi^+ \pi^-$ , has a mass of  $3872.0 \pm 0.6(\text{stat}) \pm 0.5(\text{syst}) \text{ MeV}/c^2$  and width  $\Gamma < 2.3 \text{ MeV}$  at the 90% C.L. The signal has a statistical significance of  $10.3 \sigma$ .

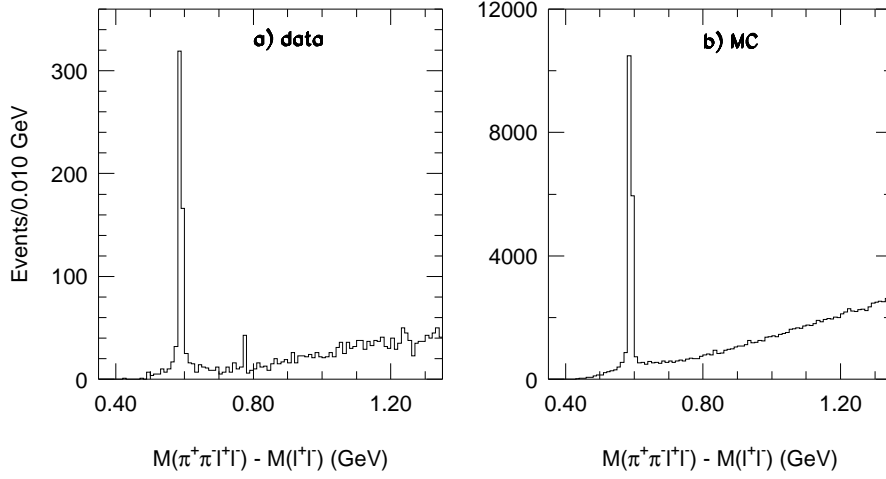


Figure 11: *Distribution of  $M(\pi^+\pi^-l^+l^-) - M(l^+l^-)$  for Belle (a) in data and (b) in generic  $B - \bar{B}$  Monte Carlo events.*

Fig. 12 shows the  $\pi^+\pi^-$  mass distribution for events in a  $\pm 5$  MeV window around the X(3872) peak. The  $\pi^+\pi^-$  invariant masses tend to cluster near the kinematic boundary, which is around the  $\rho$  mass; the entries below the  $\rho$  are consistent with background. Charmonium decays to  $\rho J/\psi$  violate isospin and are expected to be suppressed.

Belle has compared as well the rates of X and  $\psi(2S)$  production in B decays. They determined the ratio of product branching fractions for  $B^+ \rightarrow K^+ X(3872)$ ,  $X(3872) \rightarrow J/\psi \pi^+ \pi^-$  and  $B^+ \rightarrow K^+ \psi(2S)$ ,  $\psi(2S) \rightarrow J/\psi \pi^+ \pi^-$  to be  $0.063 \pm 0.012(stat) \pm 0.007(syst)$ . In an attempt to investigate the nature of this narrow state and to test the hypothesis of it being the  $1^3D_2$  or  $1^3D_3$  state, Belle has also searched for radiative transitions of the X(3872) to the  $1^3P_{1,2}$  levels. They set a 90% C.L. upper limit <sup>47)</sup>

$$\frac{\Gamma[X(3872) \rightarrow \gamma \chi_{c1}]}{\Gamma[X(3872) \rightarrow J/\psi \pi^+ \pi^-]} < 0.89. \quad (5)$$

Since the decay of  $1^3D_2$  to  $\gamma \chi_{c1}$  is an allowed  $E1$  transition with a partial width

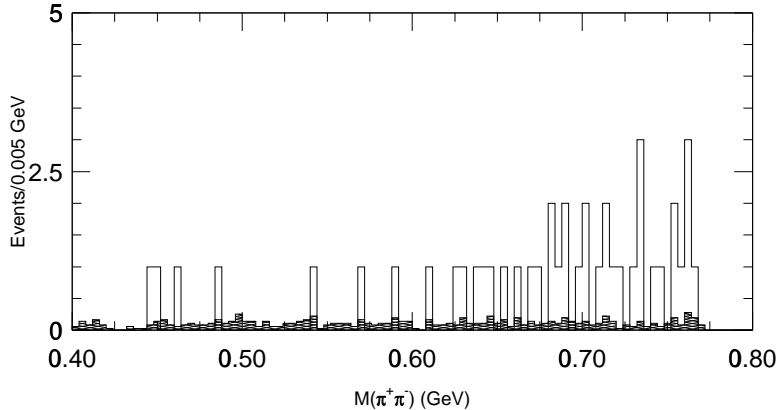


Figure 12:  $M(\pi^+\pi^-)$  distribution for events in the  $M(\pi^+\pi^-J/\psi)$  region. The shaded histogram represents sideband data normalized to the signal-box area.

which is expected to be substantially larger than that for the  $J/\psi\pi^+\pi^-$  decay, the above limit conflicts with the single-channel potential-model expectations for the  $1^3D_2$  state <sup>40</sup>). The limit <sup>48</sup>)

$$\frac{\Gamma[X(3872) \rightarrow \gamma\chi_{c2}]}{\Gamma[X(3872) \rightarrow J/\psi\pi^+\pi^-]} < 1.1, \quad (6)$$

presents problems as well for both the  $1^3D_2$  and  $1^3D_3$  interpretations.

As discussed in <sup>48</sup>) and shown in fig. 13, the Belle Collaboration presented preliminary information about the decay angular distribution of the  $J/\psi$  produced in the  $X(3872) \rightarrow J/\psi\pi^+\pi^-$  decay. The decay angular distribution of a  $J^{PC} = 1^{+-}$  state is expected to be proportional to  $\sin^2\theta$ . The  $\chi^2$  per degree of freedom for the fit in fig. 13, comparing the data with the expectation, is 75/9. This information does not determine so far  $J^{PC}$ , but it makes the  $h'_c(1^{+-})$  hypothesis very unlikely.

The hypothesis for  $X(3872)$  being the  $2^3P_1$  state was also tested. Accord-

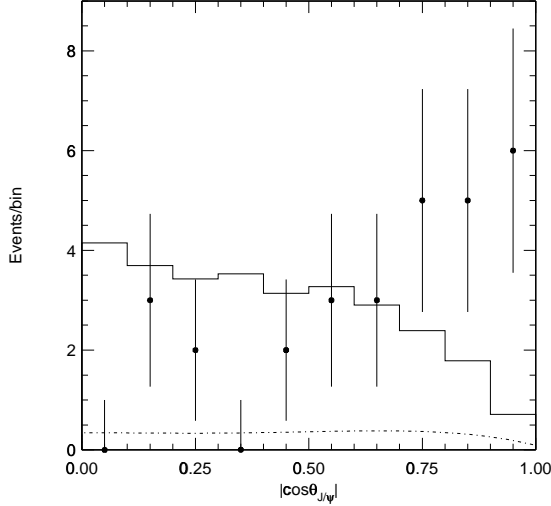


Figure 13: *Distribution of the  $|\cos|$  of the angle between the  $J/\psi$  and the kaon in the  $X$  rest frame for the decay  $B^\pm \rightarrow K^\pm \pi^+ \pi^- J/\psi$ . The dashed curve is a background contribution derived from mass sidebands on both sides of the  $X$ ; the histogram is the sum of the background and a Monte Carlo simulation for a  $J^{PC} = 1^{+-}$  state.*

ing to Ref. 49), it is expected that

$$\frac{\Gamma(2^3P_1 \rightarrow \gamma J/\psi)}{\Gamma(2^3P_1 \rightarrow J/\psi \pi^+ \pi^-) \approx \Gamma(\psi(2S) \rightarrow J/\psi \pi^0)} \approx 30. \quad (7)$$

This is based on the fact that the partial width of the channel  $2^3P_1 \rightarrow \gamma J/\psi$  is expected to be  $\Gamma(2^3P_1 \rightarrow \gamma J/\psi) \approx 11 \text{ KeV}$  and the widths of the isospin violating channels  $2^3P_1 \rightarrow J/\psi \pi^+ \pi^-$  and  $\psi(2S) \rightarrow J/\psi \pi^0$  are expected to be approximately equal to each other and very small, of the order of 0.3 KeV.

As can be seen in fig. 14, Belle found<sup>48)</sup> a small signal of  $7.7 \pm 3.6 X(3872)$  events decaying to  $J/\psi \gamma$  and set a limit of

$$\frac{Br[X(3872) \rightarrow \gamma J/\psi]}{Br[X(3872) \rightarrow J/\psi \pi^+ \pi^-]} < 0.4. \quad (8)$$

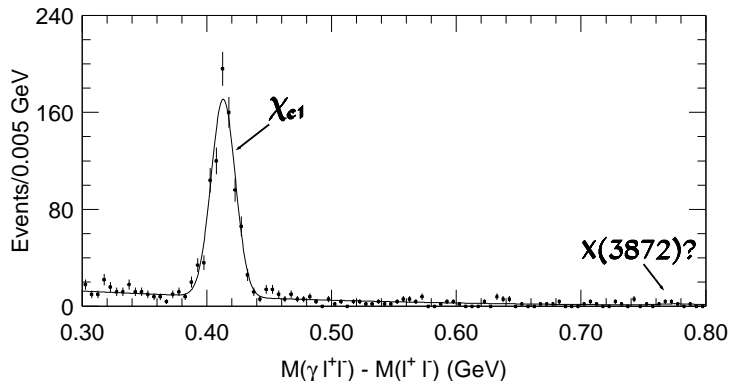


Figure 14: *The  $M(\gamma l^+ l^-) - M(l^+ l^-)$  mass distribution for  $l^+ l^-$  in the  $J/\psi$  mass window.*

This limit indicates that if the X(3872) were the  $2^3P_1$  state, then  $\Gamma(J/\psi\gamma)$  is too small, and the ratio of branching ratios in eq.8 is almost two orders of magnitude below the expectation.

Since the mass of the X(3872) state is above the  $D\bar{D}$  threshold, information about the  $X(3872) \rightarrow D\bar{D}$  decay rate can be useful in the determination of the quantum numbers of the X(3872) state. For the decays  $B^+ \rightarrow X(3872)K^+$  followed by  $X(3872) \rightarrow D^0\bar{D}^0$  and  $D^+D^-$ , Belle has set 90% C.L. upper limits on  $Br(B^+ \rightarrow X(3872)K^+) \times Br(X(3872) \rightarrow D\bar{D})$  of  $6 \times 10^{-5}$  and  $4 \times 10^{-5}$  respectively <sup>50</sup>. For the decay  $B^+ \rightarrow X(3872)K^+$  followed by  $X(3872) \rightarrow D^0\bar{D}^0\pi^0$  Belle has set a 90% C.L. upper limit of  $6 \times 10^{-5}$  <sup>50</sup>. This decay mode of the X(3872) is particularly interesting because its partial width is predicted to be large (perhaps 50 keV) if the X(3872) is a charm molecule. The Belle result at this point is perhaps an order of magnitude from challenging this expectation <sup>42</sup>.

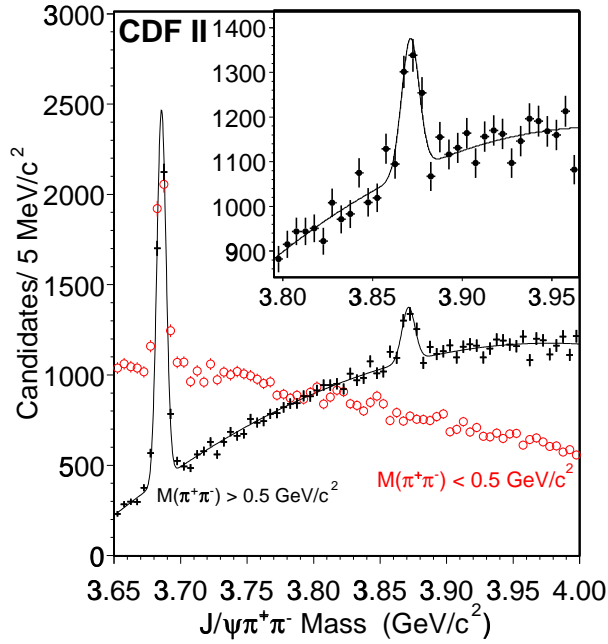


Figure 15: The mass distribution of  $J/\psi\pi^+\pi^-$  candidates with  $m(\pi^+\pi^-) > 0.5$   $\text{GeV}/c^2$  (points) and  $m(\pi^+\pi^-) < 0.5$   $\text{GeV}/c^2$  (open circles). The curve is a fit with two Gaussians and a quadratic background. The inset shows an enlargement of the high dipion-mass data and fit.

### 3.2 The X(3872) State at CDF

Using  $220 \text{ pb}^{-1}$  of data collected with the Run II detector, the CDF collaboration reported <sup>51, 52)</sup> the observation of  $730 \pm 90$  decays of a narrow state of mass  $3871.3 \pm 0.7(\text{stat}) \pm 0.4(\text{syst}) \text{ MeV}/c^2$  decaying into  $J/\psi\pi^+\pi^-$ .

The  $J/\psi\pi^+\pi^-$  mass distribution of the selected candidates is displayed in fig. 15. The open circles correspond to candidates with dipion masses smaller than  $500 \text{ MeV}/c^2$  and the solid points to dipion masses greater than  $500 \text{ MeV}/c^2$ . As noted by Belle, the dipion system of the X(3872) signal strongly favors high values, and one is unable to discern any signal in the low dipion mass plot. For dipion masses greater than  $500 \text{ MeV}/c^2$ , a large peak for the  $\psi(2S)$  is seen, and in addition, a small peak at a  $J/\psi\pi^+\pi^-$  mass around  $3872 \text{ MeV}/c^2$  is observed. The observed width of this new state is consistent with the detector resolution and the statistical significance of the signal is  $11.6 \sigma$ .

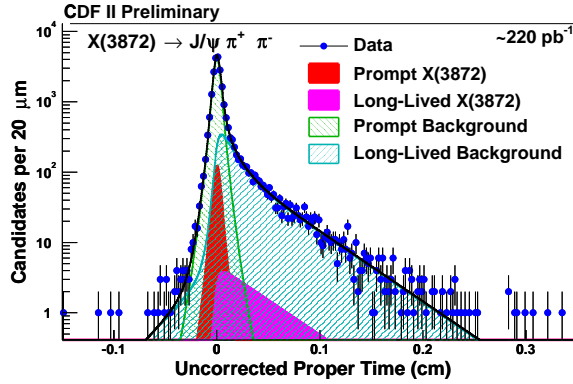


Figure 16: *Projection of the  $X(3872)$  likelihood fit onto uncorrected proper time.*

The “lifetime” distribution of  $X \rightarrow J/\psi \pi^+ \pi^-$  decays is analysed as well to quantify which fraction of this new meson arises from the decay of  $b$ -hadrons, in contrast to those produced promptly. The Tevatron can provide new information on the nature of the production mechanisms, since all relevant information from Belle is for the  $X(3872)$  produced in  $B$  decays. Fig. 16 shows the likelihood projection onto uncorrected proper time. CDF finds that  $16.1 \pm 4.9(\text{stat}) \pm 2.0(\text{syst})\%$  of the  $X$ -mesons arise from  $b$ -hadron decays, which indicates a large prompt component at the Tevatron. For comparison, they find that  $28.3 \pm 1.0(\text{stat}) \pm 0.7(\text{syst})\%$  of  $\psi(2S)$  candidates arise from such decays. The measured long-lived fraction of  $X$  is smaller than the  $\psi(2S)$  fraction but, taking into account the uncertainties, the two fractions are not very different.

### 3.3 The $X(3872)$ State at D0

Using approximately  $230 \text{ pb}^{-1}$  of data collected with the Run II detector, the D0 collaboration reported <sup>53)</sup>  $522 \pm 100$  decays of  $X(3872)$  candidates to

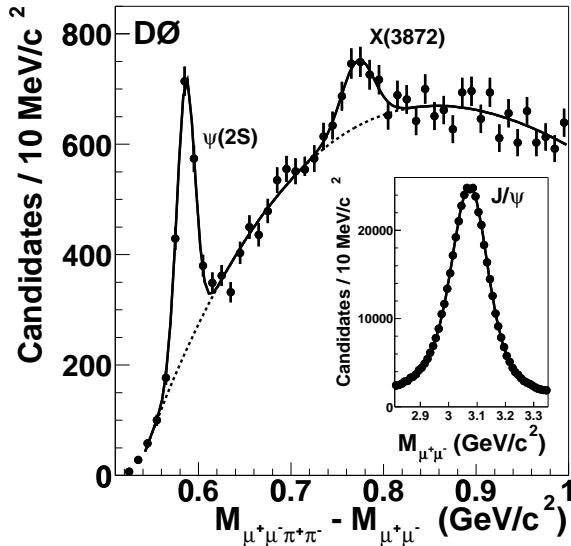


Figure 17:  $\Delta M = M(\mu^+\mu^-\pi^+\pi^-) - M(\mu^+\mu^-)$  for all candidates satisfying the selection requirements. The solid curve is a fit to the data and the dashed curve represents the background under each peak. The inset shows the mass distribution of the  $J/\psi$  candidates used in the analysis.

$J/\psi\pi^+\pi^-$  with  $m(\pi^+\pi^-) > 520 \text{ MeV}/c^2$ . Fig. 17 shows the distribution of the mass difference  $\Delta M \equiv M(\pi^+\pi^-l^+l^-) - M(l^+l^-)$  after all selections. Superimposed is a fit to the data, where the  $\psi(2S)$  and X signals are described by Gaussians and the background is described by a polynomial. The mass difference between the X(3872) state and the  $J/\psi$  is measured to be  $774.9 \pm 3.1(\text{stat.}) \pm 3.0(\text{syst.}) \text{ MeV}/c^2$  and the signal significance is determined to be approximately  $5.2 \sigma$ . D0 has investigated the production and characteristics of the X(3872) state and finds them to be similar to those of the  $\psi(2S)$  state.

### 3.4 The X(3872) State at BaBar

Using a data set of 117 M  $\Upsilon(4S) \rightarrow B\bar{B}$  decays, the BaBar Collaboration reported <sup>54)</sup> the observation of  $25.4 \pm 8.7$  X(3872) candidates. Fig. 18 shows

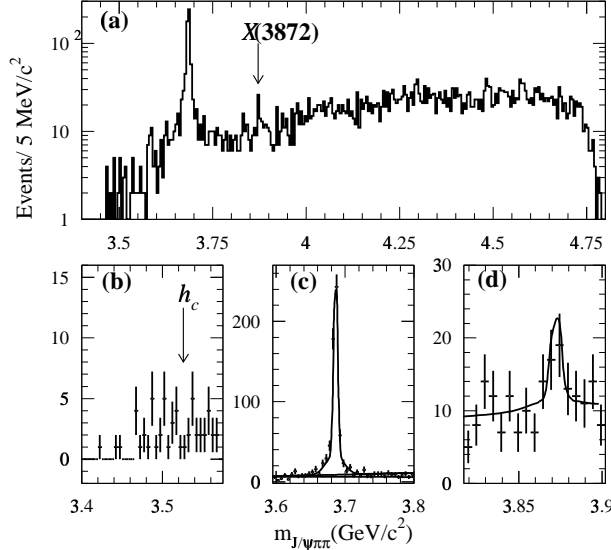


Figure 18: Distribution of  $m_{J/\psi\pi^+\pi^-}$  (a) in the entire range, (b) in the  $h_c$  region, (c) at the  $\psi(2S)$ , and (d) in the region of the  $X(3872)$  with the projection of the unbinned likelihood fit superimposed.

the  $J/\psi\pi^+\pi^-$  mass distribution in the entire range as well as in specific areas of interest, that is the  $h_c$ ,  $\psi(2S)$  and  $X(3872)$  mass regions. The mass of the  $X(3872)$  state was determined to be equal to  $3873.4 \pm 1.74 \text{ MeV}/c^2$ , consistent with the measurements of Belle, CDF and D0. The average mass based on all four experimental measurements is determined to be equal to  $3871.9 \pm 0.6 \text{ MeV}/c^2$ .

If the  $X(3872)$  is a conventional charmonium state, its decays may be similar to the ones of the  $\psi(2S)$ , which decays into  $J/\psi\pi^+\pi^-$  and, with a factor of ten smaller relative rate, into  $J/\psi\eta$ . If instead, it is hybrid charmonium state, it is also predicted<sup>46)</sup> to decay into  $J/\psi\pi^+\pi^-$  and  $J/\psi\eta$ , and the latter mode may have an enhanced rate<sup>42)</sup> if there are gluonic couplings in the  $\eta$ . Using a data set of 90 M  $\Upsilon(4S) \rightarrow B\bar{B}$  decays, the BaBar Collaboration searched for the decay  $B \rightarrow X(3872)K$ ,  $X(3872) \rightarrow J/\psi\eta$  and the resulting  $J/\psi\eta$  mass distribution is shown in fig. 19. There is possible evidence for the

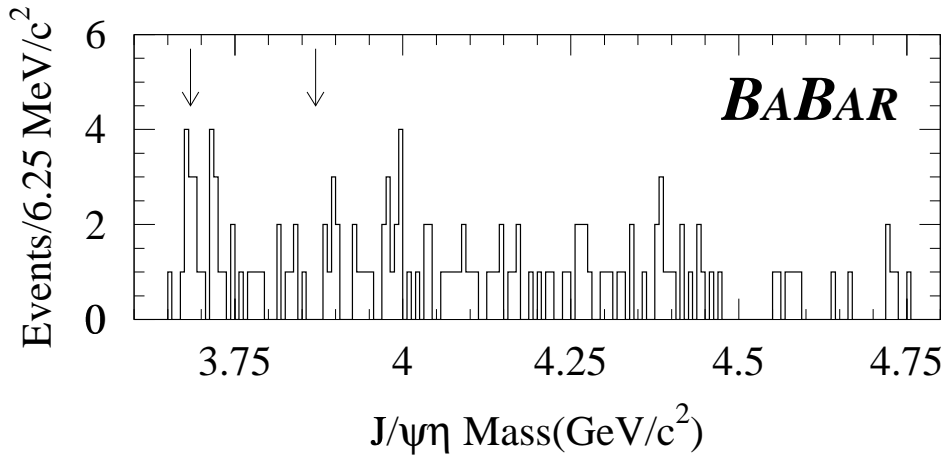


Figure 19: *The summed  $J/\psi\eta$  mass distributions from  $B^\pm \rightarrow J/\psi\eta K^\pm$  and  $B^0 \rightarrow J/\psi\eta K_S^0$ . The arrows indicate where the  $\psi(2S)$  and  $X(3872)$  signals would appear.*

$\psi(2S)$  but no evidence for the  $X(3872)$  and they determined an upper limit of  $Br(B^\pm \rightarrow X(3872)K^\pm \rightarrow J/\psi\eta K^\pm) < 7.7 \times 10^{-6}$  at 90% C.L. <sup>55</sup>). This result is consistent with the charmonium interpretation of the  $X(3872)$  and restricts the magnitude of possible enhancements with hybrid states.

#### 4 Conclusions-Prospects

In this paper we have presented results on cross sections, polarization and spectroscopy of quarkonia from measurements at hadron-hadron, lepton-hadron and lepton-lepton collisions. The study of quarkonia has proven so far to be a very interesting and challenging ground for QCD and QCD inspired models. Several new analyses have become available during the past year. Although the theory so far has been able to describe several features of quarkonia production, there are discrepancies with theoretical expectations in many of the above measurements (e.g most experimental cross sections are higher than the theoretical

predictions). Some of these measurements are currently limited by statistics.

For the Fermilab Tevatron, Run II is well underway. Approximately  $1.4(8.5) \text{ fb}^{-1}$  of data is expected by the end of FY05(FY09). The CDF and D0 experiments will increase their statistics by factors of 14 to 90 in comparison to Run I. With their better muon and silicon coverage and improved trigger capabilities, they are expected to provide improved as well as additional measurements on quarkonia production and spectroscopy which can shed light on the production mechanisms and test various theoretical expectations on masses and decay properties.

After the recent HERA upgrades, the H1 and Zeus experiments are also expected to collect additional data sets of approximately  $100 \text{ pb}^{-1}$  by the summer of 2004 and further increases in the following years. HERA-II is expected to deliver  $0.75 \text{ fb}^{-1}$  equally distributed over charges and helicities by the end of 2007. Particular effort will be made to reach  $1 \text{ fb}^{-1}$ . The upgrades may allow for polarized  $e^\pm$  beams and the additional data will certainly allow for measurements at larger  $Q^2$  and  $p_T$ .

Belle is expected to have  $500 \text{ fb}^{-1}$  by the end of 2006 and  $1 \text{ ab}^{-1}$  by the end of 2008, that is approximately 1 B  $b\bar{b}$  pairs. BaBar is also expected to have  $500 \text{ fb}^{-1}$  by the end of 2006.

Hopefully improved and more detailed calculations will become available in parallel, and a better understanding of higher order corrections will allow to address current and future problems.

The next few years will continue to be extremely interesting and challenging for the study of the Heavy Quarkonium system.

## 5 Acknowledgements

I would like to thank the conference organizers for a very productive meeting as well as Alessandro Bertolin, Tim Gershon, Vivek Jain, Rick Van Kooten, Andreas Meyer, Paul Newman, Steve Olsen, Enrico Robutti and Torsten Zeuner for discussions of their experimental data.

## References

1. F. Abe *et al*, Phys. Rev.Lett.**79** 572 (1997).
2. F. Abe *et al*, Phys. Rev.Lett.**79** 578 (1997).
3. M. Cacciari, M. Greco, Phys. Rev. Lett.**73**, 1586 (1994); E. Braaten *et al*, Phys. Lett.**B333**, 548 (1994); D.P. Roy and K. Sridhar, Phys. Lett.**B339**, 141 (1994).
4. G. Bodwin, E. Braaten and G. Lepage, Phys. Rev.**D51**, 1125 (1995) (Erratum *ibid* **55**, 5853 (1997); E. Braaten and S. Fleming, Phys. Rev.Lett.**74**

- 3327 (1995); M. Cacciari *et al*, Phys. Lett.B**356**, 553 (1995); E. Braaten and Y. Chen, Phys. Rev.D**54**, 3216 (1996).
5. P. Cho and A.K. Leibovich, Phys. Rev.D**53**, 150 (1996); P. Cho and A.K. Leibovich, Phys. Rev.D**53**, 6203 (1996).
  6. D. Acosta *et al*, Phys. Rev.Lett.**88**, 161802 (2002).
  7. T. Affolder *et al*, Phys. Rev.Lett.**85**, 2886 (2000).
  8. E. Braaten, S. Fleming, A.K. Leibovich, Phys. Rev.D**63** 094006 (2001).
  9. The CDF Collaboration,  
<http://www-cdf.fnal.gov/physics/new/bottom/bottom.html>
  10. The D0 Collaboration,  
[http://www-d0.fnal.gov/Run2Physics/ckm/approved\\_results/approved\\_results.html](http://www-d0.fnal.gov/Run2Physics/ckm/approved_results/approved_results.html);  
<http://www-d0.fnal.gov/Run2Physics/ckm/Moriond2003/index2.html>.
  11. M. Cacciari, S. Frixione, M. L. Mangano, P. Nason, G. Ridolfi, JHEP **0407** (2004) 033.
  12. The D0 Collaboration, D0 Conference Note 4523, <http://www-d0.fnal.gov/Run2Physics/WWW/results/B/B09/B09.pdf>.
  13. T. Affolder *et al*, Phys. Rev.Lett.**86**, 3963 (2001).
  14. T. Affolder *et al*, Phys. Rev.Lett.**85**, 2886 (2000).
  15. E. Braaten, B.A. Kniehl, J. Lee, Phys. Rev.D**62**, 094005 (2000).
  16. E. Braaten and J. Lee, Phys.Rev. D**65** 034005 (2002).
  17. C.N. Brown *et al*, Phys. Rev.Lett.**86**, 2529 (2001).
  18. A. Kharchilava *et al*, Phys.Rev. D**59** 094023 (1999); A. Tkabladze, Phys. Lett.B**462**, 319 (1999).
  19. ALEPH Collaboration, CERN-OPEN-99-343 Prepared for International Europhysics Conference on High-Energy Physics (HEP 97), Jerusalem, Israel, 19-26 Aug. 1997.
  20. P. Abreu *et al*, Phys. Lett.B **341** 109 (1994).
  21. M. Wadhwa, Nucl. Phys. Proc. Suppl. **64** 441 (1998).
  22. G. Alexander *et al*, Phys. Lett.B **384** 343 (1996).

23. S. Todorova-Nova, hep-ph/0112050.
24. J. Abdallah *et al*, Phys. Lett.B **565** 76 (2003).
25. M. Klasen, B. A. Khniel, L.N. Mihaila and M. Steinhauser, Phys. Rev.Lett.**89** 032001 (2002).
26. C. Adloff *et al*, Eur. Phys.J.C**25**, 25 (2002); C. Adloff *et al*, Eur. Phys.J.C**25** 1, 41 (2002).
27. S. Chekanov *et al*, Eur. Phys.J.C**27**, 173 (2002).
28. M. Krämer, Prog. Part. Nucl. Phys.**47** 141 (2001).
29. B.A. Kniehl and L. Zwirner, Nucl.Phys.B **621** 337 (2002).
30. K. Abe *et al*, Phys. Rev.Lett.**88**, 052001 (2002).
31. B. Aubert *et al*, Phys. Rev.Lett.**87**, 162002 (2001).
32. K. Abe *et al*, BELLE-CONF-0331, contributed paper, EPS 2003, Aachen, Germany, 2003.
33. P.L. Cho and A.K. Leibovich, Phys.Rev. D**54** 6690 (1996).
34. F. Yuan, C.F. Qiao and K.T. Chao, Phys.Rev. D**56** 321 (1997).
35. S. Baek, P. Ko, J. Lee and H.S. Song, Phys. Lett.B **389** 609 (1996).
36. E. Braaten and J. Lee, Phys.Rev. D**67** 054007 (2003).
37. K.Y. Liu, Z.G. He, K.T. Chao, Phys. Lett.B **557** 45 (2003).
38. G.T. Bodwin, J. Lee, E. Braaten, Phys. Rev.Lett.**90**, 162001 (2003).
39. K. Abe *et al*, hep-ex/0407009.
40. E.J. Eichten, K. Lane, C. Quigg, Phys. Rev.Lett.**89**, 162002 (2002).
41. E.J. Eichten, K. Lane, C. Quigg, Phys. Rev. D**69** 094019 (2004).
42. C. Quigg, This Volume, (2004),  
<http://www.pi.infn.it/lathuile/2004/talks/contributi/quigg.pdf>.
43. S. Pakvasa and M. Suzuki, Phys. Lett.B **579** 67 (2004).
44. F.E. Close and P.R. Page, Phys. Lett.B **578** 119 (2004).
45. M.B. Voloshin, Phys. Lett.B **579** 316 (2004).

46. F.E. Close and S. Godfrey, Phys. Lett.B **574** 210 (2003).
47. S.-K. Choi *et al*, Phys. Rev.Lett.**91**, 262001 (2003).
48. S.-K. Choi, [http://www.phys.hawaii.edu/solsen/x3872/lake\\_louise\\_2004.pdf](http://www.phys.hawaii.edu/solsen/x3872/lake_louise_2004.pdf).
49. T. Barnes and S. Godfrey, Phys. Rev.D**69**, 054008 (2004).
50. R. Chistov *et al*, Phys. Rev.Lett.**93**, 051803 (2004).
51. D.Acosta *et al*, Phys. Rev.Lett.**93**, 072001 (2004).
52. The CDFII Collaboration,  
<http://www-cdf.fnal.gov/physics/new/bottom/040624.blessed-xlonglived/>.
53. V.M. Abazov *et al*, FERMILAB-Pub-04/061-E.
54. B. Aubert *et al*, hep-ex/0406022.
55. B. Aubert *et al*, hep-ex/0402025.